

Structures of Hydrated Oxygen Anion Clusters: DFT Calculations for $\text{O}^-(\text{H}_2\text{O})_n$, $\text{O}_2^-(\text{H}_2\text{O})_n$, and $\text{O}_3^-(\text{H}_2\text{O})_n$ ($n = 0-4$)

Takamasa Seta,* Mitsuo Yamamoto, Masateru Nishioka, and Masayoshi Sadakata

Department of Chemical System Engineering, School of Engineering, The University of Tokyo, 7-3-1 Hongo, Bunkyo-ku, Tokyo 113-8656, Japan

Received: October 9, 2002; In Final Form: December 17, 2002

The complicated geometries of hydrated anion clusters are investigated using density functional calculations. The structures of the first solvation shell of $\text{O}^-(\text{H}_2\text{O})_n$, $\text{O}_2^-(\text{H}_2\text{O})_n$, and $\text{O}_3^-(\text{H}_2\text{O})_n$ ($n = 0-4$) were calculated at the B3LYP/aug-cc-pVDZ level, focusing on the hydrogen bond distances between the anion and the water, the change of the water O–H bond lengths, and the H–O–H angles for these species systematically. These parameters are related to the binding energy between the anion and the water, and the binding energy tends to decrease as the number of water molecules and the size of anions increase. Three kinds of interactions in these clusters were found as follows: (i) the strong anion–water interaction; (ii) the water–water interaction; and (iii) the weak anion–water interaction. The strong anion–water interactions are seen in all of the species. However, the water–water interactions are seen only in $\text{O}_2^-(\text{H}_2\text{O})_2$ with C_1 symmetry, $\text{O}_2^-(\text{H}_2\text{O})_3$, and $\text{O}_2^-(\text{H}_2\text{O})_4$, and the weak anion–water interactions are seen only in $\text{O}_3^-(\text{H}_2\text{O})_n$. These geometrical parameters are important to understand the structures of hydrated anions. Furthermore, the standard thermodynamic functions for $\text{X}^-(\text{H}_2\text{O})_{n-1} + \text{H}_2\text{O} \rightarrow \text{X}^-(\text{H}_2\text{O})_n$ ($\text{X} = \text{O}, \text{O}_2$, and O_3) were calculated to investigate their stability in the atmosphere. $-\Delta H^\circ$ and $-\Delta G^\circ$ decrease as the number of water molecules and the size of the anion increase. These thermodynamic functions are useful to understand the anion hydration.

Introduction

The chemistry of hydrated ionic clusters is important both in the gas phase and in the aqueous solution. Although the structures of hydrated cation clusters are well-known, such as $\text{H}^+(\text{H}_2\text{O})_n^1$ or $\text{NH}_4^+(\text{H}_2\text{O})_n^2$, the structures of anion clusters are not. It is difficult to predict the structures of anions because various geometries for the hydrates of anions exist. Recently, numerous experimental^{3–10} and theoretical^{11–17} studies of the hydrated anion clusters have been conducted. It is proved that anion–water interaction is different from cation–water interaction, which is very important to understand the structures of anion clusters. For instance, the complex between the anion and the one water molecule is not symmetrical. While the cation binds an oxygen atom of water, the anion binds only a single hydrogen atom, as shown in Figure 1. Both water–anion and water–water interactions lead to the complicated structures of the hydrated anion clusters.

Oxygen anions and their clusters, such as $\text{O}^-(\text{H}_2\text{O})_n$, $\text{O}_2^-(\text{H}_2\text{O})_n$, and $\text{O}_3^-(\text{H}_2\text{O})_n$, are important species in atmospheric chemistry, plasma chemistry, and biochemical systems. These anion clusters are also related to the neutral oxywater and hydrated oxygen cation clusters.^{18–21} Several experimental studies of oxygen anion hydration have been conducted.^{3,22–24} The mass spectra of $\text{OH}^-(\text{H}_2\text{O})_n$, $\text{O}^-(\text{H}_2\text{O})_n$, $\text{O}_2^-(\text{H}_2\text{O})_n$, and $\text{O}_3^-(\text{H}_2\text{O})_n$ ($n = 0-59$) were obtained by the discharge ionization of a He/ H_2O mixture and a flow tube reactor at about 20 Torr. Large clusters appear only when the temperature is decreased to below about 140 K. At room temperature, the number of hydrates extends only up to about 4.³ The hydration energies and the rate constants of the oxygen anions have been

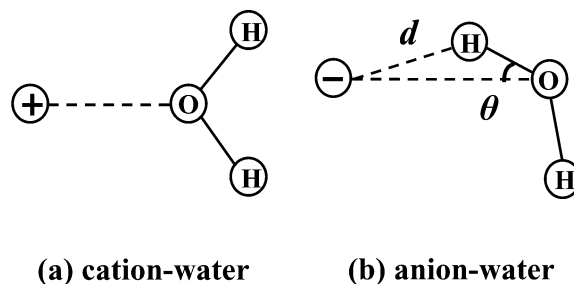


Figure 1. Starting geometries of the ion–water systems. (a) The complex between the cation and the one water molecule; (b) the complex between the anion and the one water molecule. Bond length d and bond angle θ between the anion and the water molecule are defined.

measured.^{22–24} The gas phase reaction rates of hydration, such as $\text{O}^- + \text{H}_2\text{O} + \text{M} \rightarrow \text{O}^-(\text{H}_2\text{O}) + \text{M}$, are so high that the equilibria of these reactions are achieved rapidly. Therefore, the reaction enthalpies and the free energies are very important. However, the thermodynamic functions for the hydration of O^- and O_3^- are not sufficiently known. To understand their stability and reactivity, it is necessary to know their structures. However, there are a few quantum chemical calculations on the geometries for $\text{O}^-(\text{H}_2\text{O})_n$ ^{25–29} and $\text{O}_2^-(\text{H}_2\text{O})_n$,^{30,31} and there is no calculation on that of $\text{O}_3^-(\text{H}_2\text{O})_n$.

The purpose of this study is to investigate the structures of $\text{O}^-(\text{H}_2\text{O})_n$, $\text{O}_2^-(\text{H}_2\text{O})_n$, and $\text{O}_3^-(\text{H}_2\text{O})_n$ systematically. In the calculation, only the first solvation shell around oxygen anions is considered. First, the results of geometry optimizations for $\text{O}^-(\text{H}_2\text{O})_n$, $\text{O}_2^-(\text{H}_2\text{O})_n$, and $\text{O}_3^-(\text{H}_2\text{O})_n$ are presented. The relationship between anion–water binding energies per water molecule D_0 and the number of waters or the size of anions is investigated. In the next section, the standard thermodynamic

* To whom correspondence should be addressed. E-mail: seta@env-lab.t.u-tokyo.ac.jp.

TABLE 1: Total Energies^a for H₂O, O⁻(H₂O)_n, O₂⁻(H₂O)_n, and O₃⁻(H₂O)_n (n = 0–4)

species	total energy	species	total energy
H ₂ O	-76.423 417	O ₂ ⁻ (H ₂ O) ₂ (C _{2v})	-303.267 813
O ⁻	-75.138 730	O ₂ ⁻ (H ₂ O) ₂ (C ₁)	-303.267 749
O ⁻ (H ₂ O)	-151.602 662	O ₂ ⁻ (H ₂ O) ₃	-379.711 168
O ⁻ (H ₂ O) ₂ C _s	-228.057 132	O ₂ ⁻ (H ₂ O) ₄	-456.151 770
O ⁻ (H ₂ O) ₂ (C _{2v} - 1)	-228.057 126	O ₃ ⁻	-225.544 513
O ⁻ (H ₂ O) ₂ (C _{2v} - 2)	-228.056 653	O ₃ ⁻ (H ₂ O)	-301.992 410
O ⁻ (H ₂ O) ₃	-304.504 525	O ₃ ⁻ (H ₂ O) ₂ (C _s)	-378.433 732
O ⁻ (H ₂ O) ₄	-380.943 435	O ₃ ⁻ (H ₂ O) ₂ (C ₂)	-378.433 596
O ₂ ⁻	-150.367 081	O ₃ ⁻ (H ₂ O) ₃	-454.872 110
O ₂ ⁻ (H ₂ O)	-226.821 012	O ₃ ⁻ (H ₂ O) ₄	-531.306 512
O ₂ ⁻ (H ₂ O) ₂ (C _{2h})	-303.268 914		

^a Calculated by B3LYP/aug-cc-pVDZ. All of the values are reported in hartree (0 K).

functions for X⁻(H₂O)_{n-1} + H₂O → X⁻(H₂O)_n (X = O⁻, O₂⁻, and O₃⁻) are shown to investigate their stability in the atmosphere. We compared these results to those of previous experimental or theoretical works.

Computational Methods

We used the GAUSSIAN98 package³² for all of the calculations. The density functional theory (DFT) is suitable in terms of both accuracy and computational speed. The structures of O⁻(H₂O)_n, O₂⁻(H₂O)_n, and O₃⁻(H₂O)_n were optimized at the B3LYP/aug-cc-pVDZ level.^{33,34} Zero-point energies were also calculated at the B3LYP/aug-cc-pVDZ level.

Binding energy per water molecule (*D*₀) between the anion and the water molecule was calculated by

$$D_0 \cdot n = E_c^0(X^-(H_2O)_n) - E_c^0(X^-) - n \cdot E_c^0(H_2O) \quad (1)$$

*E*_c⁰ stands for the total energy with the zero-point correction, and *n* stands for the number of water molecules. We calculated the standard enthalpy (ΔH°) and Gibbs free energy (ΔG°) at 298.15 K and 1 atm for gas phase reactions, X⁻(H₂O)_{n-1} + H₂O → X⁻(H₂O)_n (X = O, O₂, and O₃) at the B3LYP/aug-cc-pVDZ level. The standard reaction entropy (ΔS°) was calculated by the following relationship

$$\Delta G^\circ = \Delta H^\circ - T\Delta S^\circ \quad (2)$$

To assess the accuracy of calculations, we calculated the reaction enthalpy of O⁻ + H₂O + M → O⁻(H₂O) + M with various theoretical methods and compared it with experimental data. HF/aug-cc-pVDZ, BLYP/aug-cc-pVDZ, B3LYP/6-31G(d), B3LYP/6-311++G(d,p), B3LYP/cc-pVDZ, B3LYP/aug-cc-pVDZ, and B3LYP/aug-cc-pVTZ levels were used in the calculation of the reaction enthalpy.

Results

Table 1 shows the total energies of all of the species. First, the structures of a water molecule were calculated. The O–H bond distance is 0.965 Å, and the H–O–H bond angle is 104.7°. These are in good agreement with the major experimental data. The structures of all species have been optimized at the B3LYP/aug-cc-pVDZ level in this study.

O⁻(H₂O)_n. The optimized geometries of O⁻(H₂O)_n are shown in Figure 2. Figure 2a shows the stable geometry of O⁻(H₂O) with C_s symmetry. O⁻ binds only one hydrogen atom. This result corresponds to previous theoretical calculations such as MP2/6-31G(d)³⁵ and MP2/6-31+G(d,p).²⁸ The water forms a hydrogen bond with O⁻ at a distance of 1.471 Å. The water O–H bond interacting with O⁻ (1.076 Å) is longer than the

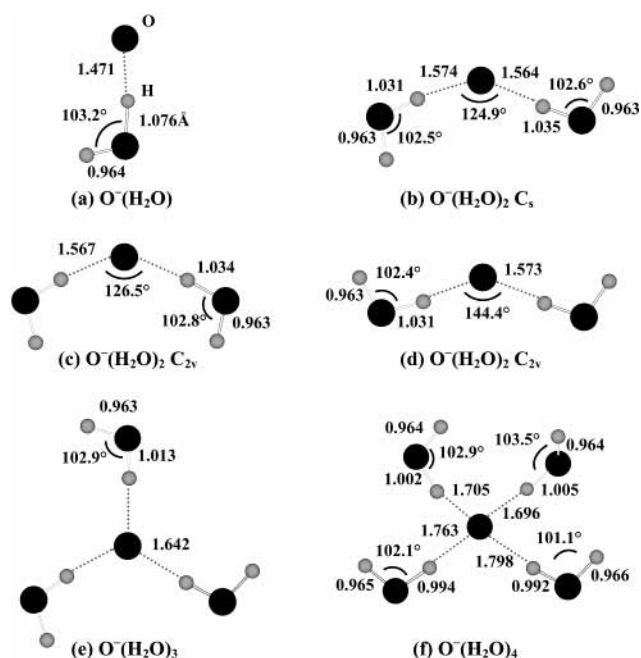


Figure 2. Optimized geometries of hydrated atomic oxygen anions: (a) O⁻(H₂O); (b) O⁻(H₂O)₂, the most stable geometry that has C_s symmetry; (c) O⁻(H₂O)₂, the stable C_{2v} geometry lying 0.02 kJ/mol above the C_s geometry; (d) O⁻(H₂O)₂, the stable C_{2v} geometry lying 1.26 kJ/mol above the C_s geometry; (e) O⁻(H₂O)₃; (f) O⁻(H₂O)₄.

free O–H bond (0.964 Å). The free O–H bond distance is almost the same as that of the single water molecule. The water H–O–H angle (103.2°) is less than that of the single water molecule (104.7°).

Three stable geometries for O⁻(H₂O)₂ were found. The most stable structure has the C_s symmetry, as shown in Figure 2b. Figure 2c indicates the C_{2v} geometry lying only 0.02 kJ/mol above the C_s symmetry, and Figure 2d shows the C_{2v} geometry lying 1.26 kJ/mol above the C_s symmetry. The hydrogen bond distances between O⁻ and waters are in the range of 1.564–1.574 Å. These are longer than that of O⁻(H₂O), which indicates that the hydrogen bonds for O⁻(H₂O)₂ are weaker than those for O⁻(H₂O). Similarly, the interacting O–H distances of O⁻(H₂O)₂ (from 1.031 to 1.035 Å) are shorter than that of O⁻(H₂O) (1.076 Å). These three geometries have been previously investigated at the MP2/6-31+(d,p) level.²⁸ The MP2 calculation also indicates that these three geometries lie within 2 kJ/mol, which is in good agreement with our calculation.

Figure 2e shows the geometry of O⁻(H₂O)₃ with C_{3h} symmetry. This geometry is considered to be generated from the attachment of a water molecule to O⁻(H₂O)₂ with C_s symmetry. The hydrogen bond distance is 1.642 Å, which is longer than that of O⁻(H₂O)₂, and the interacting O–H distance (1.013 Å) is shorter than that of O⁻(H₂O)₂. The free O–H distances are almost the same as those of the single water molecule. Although the possible symmetrical D_{3h} structure of O⁻(Ar)₃ is destroyed by the Jahn–Teller effect,³⁶ O⁻(H₂O)₃ maintains its C_{3h} symmetry. Figure 2f shows the structure of O⁻(H₂O)₄. This is a nonplanar structure. The hydrogen bond distances are longer, and the ionic O–H lengths are shorter than those of the previous clusters. There is a possibility that O⁻(H₂O)₄ contains a second solvated water molecule. However, only the first solvation shell for the O⁻(H₂O)₄ structure was considered. Jensen calculated the clusters with five or six water molecules.²⁸ He concluded that there are only four water molecules in the first solvation shell and the additional water molecules move into the second solvation.

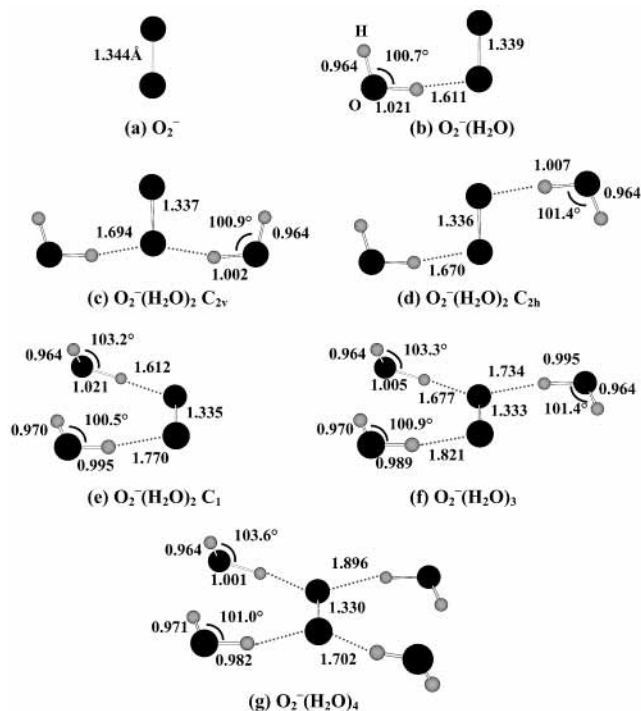


Figure 3. Optimized structures of hydrated superoxide anions: (a) O_2^- ; (b) $\text{O}_2^-(\text{H}_2\text{O})$; (c) $\text{O}_2^-(\text{H}_2\text{O})_2$, the stable C_{2v} geometry lying 2.89 kJ/mol above the C_{2h} geometry; (d) $\text{O}_2^-(\text{H}_2\text{O})_2$, the most stable geometry that has C_{2h} symmetry; (e) $\text{O}_2^-(\text{H}_2\text{O})_2$, the stable C_1 geometry lying 3.06 kJ/mol above the C_{2h} geometry; (f) $\text{O}_2^-(\text{H}_2\text{O})_3$; (g) $\text{O}_2^-(\text{H}_2\text{O})_4$.

$\text{O}_2^-(\text{H}_2\text{O})_n$. Figure 3a shows the structure of the superoxide anion, O_2^- . The O–O distance is 1.344 Å. This value is in good agreement with experimental data (1.347 Å)³⁷ and high-level ab initio calculations such as CCSD/aug-cc-pVDZ³⁸ (1.352 Å) and QCISD/aug-cc-pVDZ³⁸ (1.353 Å).

The stable geometry of $\text{O}_2^-(\text{H}_2\text{O})$ has C_s symmetry, as shown in Figure 3b. Like $\text{O}^-(\text{H}_2\text{O})$, O_2^- binds only one hydrogen atom and the other O–H bond is free. The hydrogen bond distance (1.611 Å) is longer than that of $\text{O}^-(\text{H}_2\text{O})$ (1.471 Å). This means that the binding energy between O_2^- and H_2O is weaker than that of $\text{O}^-(\text{H}_2\text{O})$. The water O–H bond length interacting with O_2^- is 1.021 Å. This is longer than that of the single water molecule (0.964 Å) but shorter than that of $\text{O}^-(\text{H}_2\text{O})$ (1.076 Å).

Three stable geometries of $\text{O}_2^-(\text{H}_2\text{O})_2$ were found, as shown in Figures 3c–e. The most stable geometry has C_{2v} symmetry. The two water molecules of the C_{2v} structure bind the same oxygen atom of O_2^- . The C_{2v} geometry lies 2.89 kJ/mol above the C_{2h} geometry, where two waters of the C_{2v} structure attach to different oxygen atoms of O_2^- . The water–water interaction is seen only in the C_1 geometry lying 3.06 kJ/mol above the C_{2h} geometry. The distance of the water O–H bond interacting with another water (0.970 Å) is longer than that of the single water molecule (0.965 Å). Weber et al. predicted the geometry of $\text{O}_2^-(\text{H}_2\text{O})_2$ using IR spectroscopy³¹ and DFT calculations at the B3LYP/6-311+G(2d,p) level. They determined that the most stable structure is the cyclic C_1 geometry, from the results of IR spectra and their DFT calculations. The C_1 geometry lies about 2 kJ/mol below the C_{2h} structure in their work, which is different from our work. However, these geometries lie within 3 kJ/mol in both results. This corresponds to a Boltzmann population ratio ($p_i/p_j = \exp(-\Delta E/RT)$) of about 3 to 1 in favor of the most stable geometry at 300 K. Therefore, these three structures may coexist.

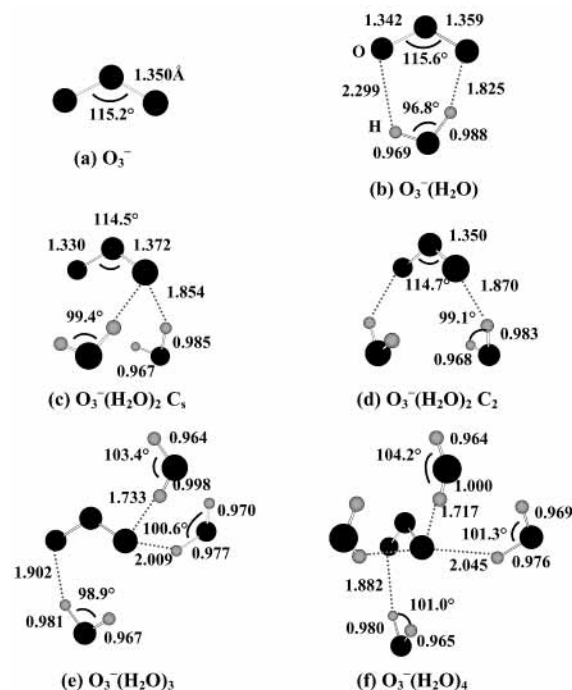


Figure 4. Optimized structures of hydrated ozone anions: (a) O_3^- ; (b) $\text{O}_3^-(\text{H}_2\text{O})$; (c) $\text{O}_3^-(\text{H}_2\text{O})_2$, the most stable geometry that has C_s symmetry; (d) $\text{O}_3^-(\text{H}_2\text{O})_2$, the stable C_2 geometry lying 0.36 kJ/mol above the C_s geometry; (e) $\text{O}_3^-(\text{H}_2\text{O})_3$; (f) $\text{O}_3^-(\text{H}_2\text{O})_4$.

Figure 3f shows the stable geometry for $\text{O}_2^-(\text{H}_2\text{O})_3$. The three hydrogen bond distances are 1.677, 1.734, and 1.821 Å. The water O–H lengths interacting with O_2^- are 1.005, 0.995, and 0.989 Å. There is a water–water interaction because the O–H length forming the water–water hydrogen bond (0.970 Å) is longer than that of normal water (0.965 Å). This structure can be generated from both $\text{O}_2^-(\text{H}_2\text{O})_2$ with C_{2h} symmetry and $\text{O}_2^-(\text{H}_2\text{O})_2$ with C_1 symmetry. $\text{O}_2^-(\text{H}_2\text{O})_4$ with C_i symmetry is drawn in Figure 3g. This structure is the same as that of previous studies.^{30,31} We considered that there are four water molecules in the first solvation shell, since Weber et al.³¹ suggested that the fifth water molecule binds to the water molecule in the tetrahydrate for the structure of $\text{O}_2^-(\text{H}_2\text{O})_5$.

$\text{O}_3^-(\text{H}_2\text{O})_n$. Figure 4 shows the optimized geometries for $\text{O}_3^-(\text{H}_2\text{O})_n$ from $n = 0$ –4. O_3^- has C_{2v} symmetry, as shown in Figure 4a. The Mulliken charge of the central oxygen atom is +0.10, and the two outside oxygen atoms are both –0.55. According to this distribution, it is expected that hydrogen atoms of water molecules bind the outside oxygen atoms.

Figure 4b shows the stable C_s geometry of $\text{O}_3^-(\text{H}_2\text{O})$. One hydrogen atom of H_2O binds strongly to the outside oxygen atom of O_3^- , and another hydrogen atom binds weakly to another outside oxygen atom of O_3^- . Unlike $\text{O}^-(\text{H}_2\text{O})$ and $\text{O}_2^-(\text{H}_2\text{O})$, there is no completely free O–H bond. The water O–H bond lengths are 0.988 and 0.969 Å. These two kinds of anion–water interactions do not exist in $\text{O}^-(\text{H}_2\text{O})_n$ and $\text{O}_2^-(\text{H}_2\text{O})_n$, and we define them as the strong anion–water interaction and the weak anion–water interaction. The strong hydrogen bond distance (1.825 Å) is longer than those of $\text{O}^-(\text{H}_2\text{O})$ (1.471 Å) and $\text{O}_2^-(\text{H}_2\text{O})$ (1.611 Å). This result indicates that the anion–water interaction of $\text{O}_3^-(\text{H}_2\text{O})$ is weaker than those of $\text{O}^-(\text{H}_2\text{O})$ and $\text{O}_2^-(\text{H}_2\text{O})$.

Two stable geometries for $\text{O}_3^-(\text{H}_2\text{O})_2$ were found, as shown in Figures 4c,d. The most stable one has C_s symmetry. Two waters bind the same oxygen atom of O_3^- . The C_2 geometry lies only 0.36 kJ/mol above the C_s geometry. Two waters of

TABLE 2: Binding Energies Per Water Molecule (D_0), Bond Lengths (d), and Bond Angles (θ) between the Anion and the Water Molecule for $O^-(H_2O)_n$, $O_2^-(H_2O)_n$, and $O_3^-(H_2O)_n$ Clusters^a

species	D_0^b	d^c	θ^d
$O^-(H_2O)$	106.37	1.471	1.46
$O^-(H_2O)_2 (C_s)$	93.95	1.569	2.18
$O^-(H_2O)_2 (C_{2v} - 1)$	93.94	1.567	1.50
$O^-(H_2O)_2 (C_{2v} - 2)$	93.32	1.573	3.41
$O^-(H_2O)_3$	83.62	1.642	2.13
$O^-(H_2O)_4$	72.88	1.741	5.05
$O_2^-(H_2O)$	80.11	1.611	4.91
$O_2^-(H_2O)_2 (C_{2h})$	72.20	1.670	2.97
$O_2^-(H_2O)_2 (C_{2v})$	70.75	1.694	6.98
$O_2^-(H_2O)_2 (C_1)$	70.67	1.691	4.30
$O_2^-(H_2O)_3$	64.62	1.744	5.51
$O_2^-(H_2O)_4$	59.74	1.799	5.71
$O_3^-(H_2O)$	64.27	1.825	11.34
$O_3^-(H_2O)_2 (C_s)$	55.64	1.854	11.81
$O_3^-(H_2O)_2 (C_2)$	55.46	1.870	12.37
$O_3^-(H_2O)_3$	50.19	1.881	11.00
$O_3^-(H_2O)_4$	44.85	1.922	11.54

^a Calculated by B3LYP/aug-cc-pVDZ. ^b Energies in kJ/mol. ^c Lengths in Ångstroms. ^d Angles in degrees.

the C_2 structure attach to different oxygen atoms of O_3^- . The C_s geometry, whose two waters attach the same oxygen atom, is more stable than the C_2 geometry. This result is different from that of $O_2^-(H_2O)_2$, where the C_{2h} geometry is more stable than the C_{2v} geometry. These two geometries have no free water O–H bond, shown that the water O–H distances (0.967 or 0.968 Å) are longer than that of the single water molecule (0.965 Å).

It was very difficult to predict the geometry of $O_3^-(H_2O)_3$. Only one geometry has been found, which has C_1 symmetry. Figure 4e shows the unsymmetrical $O_3^-(H_2O)_3$ structure. One water binds O_3^- like $O_3^-(H_2O)$, and the other two waters are located at the opposite sides. $O_3^-(H_2O)_4$ with C_s symmetry is shown in Figure 4f. This structure is considered to be generated from $O_3^-(H_2O)_3$ with C_1 symmetry. One of the hydrogen bond lengths exceeds 2 Å, which indicates that the anion–water interaction energies of $O_3^-(H_2O)_4$ are lower than those of smaller clusters.

Although O^- and O_2^- can accommodate four water molecules in the first solvation shell,^{28,31} the question is how many waters O_3^- can bind. Wang et al. calculated the structures of $NO_3^-(H_2O)_n$ clusters and found that there are only three water molecules in the first solvation shell. The fourth to sixth waters are added to the second solvation shell.⁸ It is inferred from this result that the number of the first solvated waters has a connection with not only the size but also the geometry and binding energy of the anions. Moreover, the central oxygen atom cannot bind any waters because of the charge distribution of O_3^- . So, we considered that O_3^- could accept up to four water molecules in the first solvation shell.

Discussion

Analysis of Cluster Structures. To understand these complicated geometries of anion clusters, the structural parameters were compared, such as D_0 , d , θ , and the O–H distance of water. We first considered the anion–water binding energies, D_0 . These are calculated from eq 1. Table 2 lists D_0 values of each species. D_0 has a tendency to decrease as the number of water molecules and the size of anion increase. We can say that the ion–dipole interactions of these clusters depend on the electric field of ions. Therefore, the interaction energy is inversely proportional to the size of ions. For example, D_0 of $O^-(H_2O)$ (106.37 kJ/mol) is the largest in $O^-(H_2O)_n$ and D_0 of

TABLE 3: Water Bond Lengths and Angles^a for H_2O , $O^-(H_2O)_n$, $O_2^-(H_2O)_n$, and $O_3^-(H_2O)_n$

species	length ^b		angle ^c
	H_{in}^d –O	O– H_{out}^e	H–O–H
H_2O	0.965	0.965	104.7
$O^-(H_2O)$	1.076	0.964	103.2
$O^-(H_2O)_2 (C_s)$	1.034	0.963	102.6
$O^-(H_2O)_2 (C_{2v} - 1)$	1.034	0.963	102.8
$O^-(H_2O)_2 (C_{2v} - 2)$	1.031	0.963	102.4
$O^-(H_2O)_3$	1.013	0.963	102.9
$O^-(H_2O)_4$	0.998	0.965	102.4
$O_2^-(H_2O)$	1.021	0.964	100.7
$O_2^-(H_2O)_2 (C_{2h})$	1.007	0.964	101.4
$O_2^-(H_2O)_2 (C_{2v})$	1.002	0.964	100.9
$O_2^-(H_2O)_2 (C_1)$	1.003	0.967	101.8
$O_2^-(H_2O)_3$	0.996	0.966	101.9
$O_2^-(H_2O)_4$	0.991	0.967	102.3
$O_3^-(H_2O)$	0.988	0.969	96.8
$O_3^-(H_2O)_2 (C_s)$	0.985	0.967	99.4
$O_3^-(H_2O)_2 (C_2)$	0.983	0.968	99.1
$O_3^-(H_2O)_3$	0.985	0.967	101.0
$O_3^-(H_2O)_4$	0.983	0.967	102.0

^a Calculated by B3LYP/aug-cc-pVDZ. ^b Lengths in Ångstroms. ^c Angles in degrees. ^d H_{in} stands for the hydrogen atom binding on the anion. ^e H_{out} stands for another hydrogen atom in the water molecule.

$O_3^-(H_2O)_3$ (50.19 kJ/mol) is smaller than those of $O^-(H_2O)_3$ (83.62 kJ/mol) and $O_2^-(H_2O)_3$ (64.62 kJ/mol).

We stated that the appearance of the anion–water bonds varies in each cluster. Then, the anion–water bond lengths (d) and bond angles (θ) defined in Figure 1b were investigated. The values of d and θ are listed in Table 2. These values are the average of measurements of many water molecules. The d for $O^-(H_2O)$ (1.471 Å) is the smallest for all of the species. The value of d increases as the number of water molecules and the size of anion increase. It is obvious that d has a strong negative correlation with D_0 . We also found that θ tends to increase as d increases. The strong anion–water hydrogen bond of the three atoms makes it close to linear, like $O^-(H_2O)$, whereas the weak anion–water interaction leads to a loose structure.

Next, various parameters of water molecules were focused on, such as O–H lengths or H–O–H angles. We define the hydrogen atom binding strongly with an anion as H_{in} and the other hydrogen atom as H_{out} . The distances of H_{in} –O and H_{out} –O are shown in Table 3. These values are the average of many water molecules. It is natural that the two H–O distances of single water molecule are the same (0.965 Å). H_{in} –O distances of all of the clusters are longer than those of the single water. H_{in} –O is almost proportional to D_0 .

On the other hand, there is little variety in O– H_{out} distances. All of the values are almost the same as that of a single water molecule (0.965 Å). It is noticeable that the O– H_{out} distance for $O_2^-(H_2O)_2$ with C_1 symmetry (0.967 Å) is longer than those for $O_2^-(H_2O)_2$ with C_{2h} and $O_2^-(H_2O)_2$ with C_{2v} symmetry (0.964 Å). This indicates that $O_2^-(H_2O)_2$ with C_1 symmetry has the water–water interaction in its structure, as shown in Figure 3. Similarly, the O– H_{out} distances of $O_2^-(H_2O)_3$ (0.966 Å) and $O_2^-(H_2O)_4$ (0.967 Å), which have the water–water hydrogen bonds, are relatively long. The O– H_{out} lengths of $O_3^-(H_2O)_n$ are longer than that of the single water molecule. This is the result of the weak anion–water interactions, only seen in $O_3^-(H_2O)_n$. In other words, the O– H_{out} lengths are influenced by the water–water interaction or the weak anion–water interaction. These interactions are weaker than the strong anion–

TABLE 4: Calculated ΔH° with Various Theoretical Methods for the Gas Phase Reaction $O^- + H_2O \rightarrow O^-(H_2O)$ in Comparison to the Experimental Data

method/basis set	ΔH° (kJ/mol) ^a
HF/aug-cc-pVDZ	-87.04
BLYP/aug-cc-pVDZ	-132.09
B3LYP/6-31G(d)	-187.90
B3LYP/6-311++G(d,p)	-116.08
B3LYP/cc-pVDZ	-196.77
B3LYP/aug-cc-pVDZ	-110.99
B3LYP/aug-cc-pVTZ	-109.54
exp ^b	-110

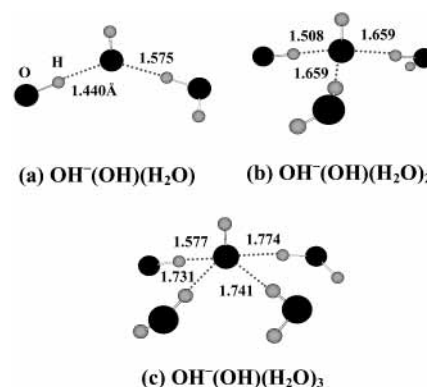
^a ΔH° stands for the standard reaction enthalpy at 298.15 K and 1 atm. ^b Ref 39.

water interaction, as shown by the little change of the O–H_{out} bond lengths.

The bond angles of waters are shown in Table 3. There is no obvious tendency in the H–O–H angles, but all of the values of clustering water (96.8–103.2°) are less than that of the single water molecule (104.7°). These transformations of water molecules mean that an electric field from the cluster anion influences the water geometry and the electronic structure.

Thermodynamics. The standard reaction enthalpy for the hydration of O^- with various theoretical methods was calculated, and the results are shown in Table 4. ΔH° is -110.99 kJ/mol with B3LYP/aug-cc-pVDZ. This value is in good agreement with experimental data.³⁹ In contrast, HF/aug-cc-pVDZ underestimates and BLYP/aug-cc-pVDZ overestimates the absolute value of ΔH° , so it is necessary to use the B3LYP method. Diffuse functions are essential for the calculations of anions, showing that B3LYP/6-31G(d) and B3LYP/cc-pVDZ overestimate the absolute value of ΔH° markedly. ΔH° values calculated with B3LYP/6-311++G(d,p), B3LYP/aug-cc-pVDZ, and B3LYP/aug-cc-pVTZ correspond to experimental data very well. B3LYP/aug-cc-pVDZ was selected in this research.

Table 5 shows the standard thermodynamic functions for gas phase reactions $O^-(H_2O)_{n-1} + H_2O \rightarrow O^-(H_2O)_n$, $O_2^-(H_2O)_{n-1} + H_2O \rightarrow O_2^-(H_2O)_n$, and $O_3^-(H_2O)_{n-1} + H_2O \rightarrow O_3^-(H_2O)_n$ at 298.15 K and 1 atm at the B3LYP/aug-cc-pVDZ level. If there are multiple structures, a thermal average was calculated. In the case of O^- , we also considered the structures of the type $OH^-(OH)(H_2O)_{n-1}$ ²⁴ to calculate the thermodynamic functions. The optimized geometries of $OH^-(OH)(H_2O)_{n-1}$ ($n = 2-4$) are shown in Figure 5. We considered only the first solvation shell. $OH^-(OH)(H_2O)$ lies 2.02 kJ/mol above the C_s symmetry of $O^-(H_2O)_2$. $OH^-(OH)(H_2O)_2$ lies 7.54 kJ/mol above the C_{3h}

**Figure 5.** Optimized structures of $OH^-(OH)(H_2O)_{n-1}$: (a) $OH^-(OH)(H_2O)$; (b) $OH^-(OH)(H_2O)_2$; (c) $OH^-(OH)(H_2O)_3$.

symmetry of $O^-(H_2O)_3$. $OH^-(OH)(H_2O)_3$ lies 5.93 kJ/mol above $O^-(H_2O)_4$. If there are any experimental data, we have compared them with our calculations. ΔH° and ΔG° values of the reaction $O_2^-(H_2O)_{n-1} + H_2O \rightarrow O_2^-(H_2O)_n$ were investigated experimentally by Arshadi and Kebarle using van't Hoff plots,²² and ΔG° values for the formation of $O_2^-(H_2O)_3$, $O_3^-(H_2O)_2$, and $O_3^-(H_2O)_3$ were studied by Fehsenfeld and Ferguson using the flowing afterglow system.²⁴ These values are in relatively good agreement with our calculations, as shown in Table 5. However, $-\Delta H^\circ$ and $-\Delta G^\circ$ in this work tend to be somewhat less than their experimental results.

Figure 6 shows $-\Delta G^\circ$ for the gas phase hydration of oxygen anions as a function of hydration number. $-\Delta G^\circ$ tends to decrease as the number of water molecules increases, such as D_0 . This means that the number of water molecules at 298.15 K and 1 atm has an upper limit. Similarly, $-\Delta G^\circ$ decreases as the size of the central anion increases. This means that the number of water molecules for $O^-(H_2O)_n$ is larger than those of $O_2^-(H_2O)_n$ and $O_3^-(H_2O)_n$. $-\Delta H^\circ$ exhibits the same tendency. This trend corresponds to the hydration of halide anions,⁴⁰ such as F^- , Cl^- , Br^- , and I^- . The ΔS° values for the hydration reactions are about -100 J/K/mol, as shown in Table 5. These reaction entropies indicate that the hydration of oxygen anions strongly correlates with temperature.

These thermodynamic functions are helpful to understand the anion hydration. The $-\Delta G_{3,4}^\circ$ values at 298.15 K for the hydration reactions of $O^-(H_2O)_n$, $O_2^-(H_2O)_n$, and $O_3^-(H_2O)_n$ are nearly thermoneutral (-10.33, -9.34, and +2.75, respectively). This result does not contradict the experimental result³

TABLE 5: Calculated^a and Experimental ΔH° , ΔG° , and ΔS° for the Gas Phase Reactions $O^-(H_2O)_{n-1} + H_2O \rightarrow O^-(H_2O)_n$, $O_2^-(H_2O)_{n-1} + H_2O \rightarrow O_2^-(H_2O)_n$, and $O_3^-(H_2O)_{n-1} + H_2O \rightarrow O_3^-(H_2O)_n$

species	$n - 1, n$	ΔH° (kJ/mol) ^b		ΔG° (kJ/mol) ^c		ΔS° (J/mol/K) ^d	
		calcd	exp	calcd	exp	calcd	exp
$O^-(H_2O)_n$	0, 1	-110.99	-110 ^e	-84.01		-90.49	
	1, 2	-84.87		-52.07		-110.04	
	2, 3	-66.79		-32.57		-114.77	
	3, 4	-44.58		-10.49		-114.33	
$O_2^-(H_2O)_n$	0, 1	-84.83	-77.0 ^f	-53.66	-52.3 ^f	-104.54	
	1, 2	-66.71	-72.0 ^f	-28.94	-41 ^f	-126.66	
	2, 3	-54.47	-64.4 ^f	-17.68	-29 ^f -22 ^g	-123.40	
	3, 4	-48.03		-9.34	-14 ^f	-129.77	
$O_3^-(H_2O)_n$	0, 1	-66.48		-34.72		-106.52	
	1, 2	-50.53		-13.18	-26 ^g	-125.30	
	2, 3	-43.19		-9.64	-19 ^g	-112.52	
	3, 4	-30.33		+2.75		-110.95	

^a Calculated by B3LYP/aug-cc-pVDZ. ^b ΔH° stands for the standard reaction enthalpy at 298.15 K and 1 atm. ^c ΔG° stands for the standard reaction Gibbs free energy at 298.15 K and 1 atm. ^d ΔS° stands for the standard reaction entropy at 298.15 K and 1 atm. ^e Ref 39. ^f Ref 22. ^g Ref 24.

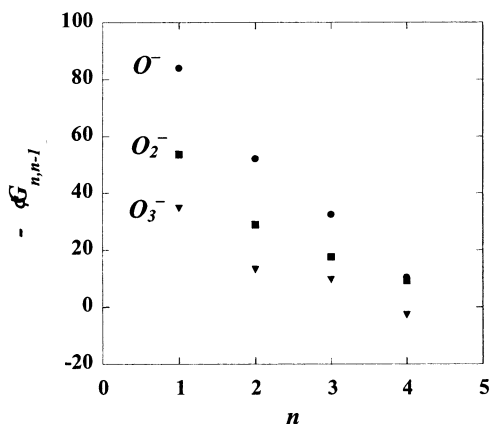


Figure 6. $-\Delta G^\circ$ at 298.15 K for the gas phase hydration of oxygen anions as a function of the hydration number.

in which the number of hydrates extends only up to about 4 at room temperature.

Conclusions

We report a theoretical study of the first solvation shell of $O^-(H_2O)_n$, $O_2^-(H_2O)_n$, and $O_3^-(H_2O)_n$. Several new structures were found in this work. To understand these complicated structures systematically, we compared the structural parameters such as anion–water binding energies, anion–water hydrogen bond distances, or water O–H distances. The binding energy per water molecule (D_0) decreases as the number of water molecules and the size of anions increase. We found that the anion–water hydrogen bond distances and the H_{in} –O lengths have a strong negative correlation with D_0 . The O– H_{out} lengths represent weaker interactions, such as water–water hydrogen bond ($O_2^-(H_2O)_2$ with C_1 symmetry, $O_2^-(H_2O)_3$, and $O_2^-(H_2O)_4$) or weak anion–water interactions ($O_3^-(H_2O)_n$). These geometrical parameters are important to understand the structures of hydrated anions. Then, we calculated the standard thermodynamic functions for $X^-(H_2O)_{n-1} + H_2O \rightarrow X^-(H_2O)_n$ ($X = O^-, O_2^-,$ and O_3^-). $-\Delta H^\circ$ and $-\Delta G^\circ$ decrease with the number of water molecules and the size of anions, same as D_0 . The ΔS° for the hydration reactions is about -100 J/K/mol. These thermodynamic functions are helpful to understand the anion hydration. Because the $-\Delta G_{3,4}^\circ$ values at 298.15 K for the hydration reactions of $O^-(H_2O)_n$, $O_2^-(H_2O)_n$, and $O_3^-(H_2O)_n$ are nearly thermoneutral, the number of water molecules is up to around 4 at room temperature.

Acknowledgment. This research was supported by JST (Japan Science and Technology Corporation) under the CREST program.

References and Notes

- (1) Khan, A. *Chem. Phys. Lett.* **2000**, *319*, 440.
- (2) Khan, A. *Chem. Phys. Lett.* **2001**, *338*, 201.

- (3) Yang, X.; Castleman, A. W., Jr. *J. Phys. Chem.* **1990**, *94*, 8500.
- (4) Yang, X.; Castleman, A. W., Jr. *J. Phys. Chem.* **1991**, *95*, 6182.
- (5) Arshadi, M.; Yamdagni, R.; Kebarle, P. *J. Phys. Chem.* **1970**, *74*, 1475.
- (6) Clements, T. G.; Luong, A. K.; Deyerl, H.; Continetti, R. E. *J. Chem. Phys.* **2001**, *114*, 8436.
- (7) Yang, X.; Wang, X.; Wang, L. *J. Chem. Phys.* **2001**, *115*, 2889.
- (8) Wang, X.; Yang, X.; Wang, L. *J. Chem. Phys.* **2002**, *116*, 561.
- (9) Ayotte, P.; Weddle, G. H.; Johnson, M. A. *J. Chem. Phys.* **1999**, *110*, 7129.
- (10) Yeh, I.; Prera, L.; Berkowitz, M. L. *Chem. Phys. Lett.* **1997**, *264*, 31.
- (11) Novoa, J. J.; Mota, F.; Perez del Valle, C.; Planas, M. *J. Phys. Chem. A* **1997**, *101*, 7842.
- (12) Roszak, S.; Kowal, M.; Gora, R. W. *J. Chem. Phys.* **2001**, *115*, 3469.
- (13) Raugei, S.; Klein, M. L. *J. Chem. Phys.* **2002**, *116*, 196.
- (14) Turki, M.; Milet, A.; Ouamerali, O.; Moszynski, R.; Kochanski, E. *THEOCHEM* **2002**, *577*, 239.
- (15) Masamura, M. *Chem. Phys. Lett.* **2001**, *339*, 279.
- (16) Perez del Valle, C.; Novoa, J. J. *Chem. Phys. Lett.* **1997**, *269*, 401.
- (17) Gora, R. W.; Roszak, S.; Leszczynski, J. *Chem. Phys. Lett.* **2000**, *325*, 7.
- (18) Schröder, D.; Schalley, C. A.; Goldberg, N.; Hrusak, J.; Schwarz, H. *Chem. Eur. J.* **1996**, *2*, 1235.
- (19) Schröder, D. *Angew. Chem., Int. Ed.* **2002**, *41*, 41.
- (20) Jursic, B. S. *THEOCHEM* **1997**, *401*, 45.
- (21) Okajima, T. *THEOCHEM* **2001**, *572*, 45.
- (22) Arshadi, M.; Kebarle, P. *J. Phys. Chem.* **1970**, *74*, 1483.
- (23) Payzant, J. D.; Kebarle, P. *J. Chem. Phys.* **1972**, *56*, 3482.
- (24) Fehsenfeld, F. C.; Ferguson, E. E. *J. Chem. Phys.* **1974**, *61*, 3181.
- (25) Hrusak, J.; Friedrichs, H.; Schwarz, H.; Razafinjanahary, H.; Chermette, H. *J. Phys. Chem.* **1996**, *100*, 100.
- (26) Jensen, S. J. K.; Klaning, U. K. *Chem. Phys. Lett.* **1995**, *241*, 404.
- (27) Jensen, S. J. K.; Csizmadia, I. G. *THEOCHEM* **1998**, *455*, 69.
- (28) Jensen, S. J. K. *THEOCHEM* **2000**, *498*, 69.
- (29) Jensen, S. J. K. *THEOCHEM* **2002**, *578*, 63.
- (30) Weber, J. M.; Kelley, J. A.; Nielsen, S. B.; Ayotte, P.; Johnson, M. A. *Science* **2000**, *287*, 2461.
- (31) Weber, J. M.; Kelley, J. A.; Robertson, W. H.; Johnson, M. A. *J. Chem. Phys.* **2001**, *114*, 2698.
- (32) Frisch, M. J.; Trucks, G. W.; Schlegel, H. B.; Scuseria, G. E.; Robb, M. A.; Cheeseman, J. R.; Zakrzewski, V. G.; Montgomery, J. A., Jr.; Stratmann, R. E.; Burant, J. C.; Dapprich, S.; Millam, J. M.; Daniels, A. D.; Kudin, K. N.; Strain, M. C.; Farkas, O.; Tomasi, J.; Barone, V.; Cossi, M.; Cammi, R.; Mennucci, B.; Pomelli, C.; Adamo, C.; Clifford, S.; Ochterski, J.; Petersson, G. A.; Ayala, P. Y.; Cui, Q.; Morokuma, K.; Malick, D. K.; Rabuck, A. D.; Raghavachari, K.; Foresman, J. B.; Cioslowski, J.; Ortiz, J. V.; Stefanov, B. B.; Liu, G.; Liashenko, A.; Piskorz, P.; Komaromi, I.; Gomperts, R.; Martin, R. L.; Fox, D. J.; Keith, T.; Al-Laham, M. A.; Peng, C. Y.; Nanayakkara, A.; Gonzalez, C.; Challacombe, M.; Gill, P. M. W.; Johnson, B. G.; Chen, W.; Wong, M. W.; Andres, J. L.; Head-Gordon, M.; Replogle, E. S.; Pople, J. A. *Gaussian 98*; Gaussian, Inc.: Pittsburgh, PA, 1998.
- (33) Becke, A. D. *J. Chem. Phys.* **1993**, *98*, 1372.
- (34) Kendall, R. A.; Dunning, T. H., Jr.; Harrison, R. A. *J. Chem. Phys.* **1992**, *96*, 6796.
- (35) Roehl, C. M.; Snodgrass, J. T.; Deakyne, C. A.; Bowers, M. T. *J. Chem. Phys.* **1991**, *94*, 6546.
- (36) Roszak, S.; Gora, R.; Leszczynski, L. *Chem. Phys. Lett.* **1999**, *313*, 198.
- (37) Huber, K. B.; Herzberg, G. *Constants of Diatomic Molecules*; Van Nostrand: New York, 1979.
- (38) Bu, Y.; Liu, C. *THEOCHEM* **1999**, *490*, 7.
- (39) Arnold, D. W.; Xu, C.; Neumark, D. M. *J. Chem. Phys.* **1995**, *102*, 6088.
- (40) Hiraoka, K.; Mizuse, S.; Yamabe, S. *J. Phys. Chem.* **1988**, *92*, 3943.